Sensors and Actuators A 237 (2016) 147–154

Contents lists available at ScienceDirect

Sensors and Actuators A: Physical

journal homepage: www.elsevier.com/locate/sna

MEMS cantilever sensor array oscillators: Theory and experiments

Sevil Zeynep Lulec[a], Ulas Adiyan[a,*], Goksen G. Yaralioglu[b], Yusuf Leblebici[c], Hakan Urey[a]

[a] Koç University, Istanbul, Turkey
[b] Özyeğin University, Istanbul, Turkey
[c] École Polytechnique Fédérale de Lausanne, Switzerland

ARTICLE INFO

Article history:
Received 20 August 2015
Received in revised form 2 November 2015
Accepted 25 November 2015
Available online 28 November 2015

Keywords:
Biosensors
MEMS cantilever sensor arrays
Multiple self-sustained oscillation
Interferometric readout
Diffraction grating

ABSTRACT

This paper demonstrates that an array of cantilever sensors can be operated simultaneously at resonance using a single actuator and a single photodetector. Self-sustained oscillations (SSOs) of cantilevers can be achieved in a feed-back loop using gain saturation mechanism in the electronics. Multiple cantilevers require separate saturation mechanisms and separate sensing electronics for each channel. We introduced optical non-linearity using diffraction gratings at the tip of each cantilever which provide separate saturation non-linearity, enabling a single detector based oscillator array. Two-cantilever SSO operation is investigated analytically, and the multiple frequency oscillation criteria are established. Cross-coupling between the oscillation frequencies has been investigated by using this multi cantilever model. The proposed model will be helpful to design dynamic-mode MEMS (Micro-electro-mechanical systems) cantilever sensor arrays with the desired functionality and cross-talk levels. This multiple SSO operation can be used in conjunction with dense cantilever arrays for various biosensor applications. Moreover, the model can also be useful to understand the operation of any kind of multiple simultaneous oscillator systems, which employs a single feed-back loop. We also present experimental results that confirm our model.

1. Introduction

The concept of self-sustained oscillation (SSO) has been commonly used to maintain oscillations of dynamic MEMS (Micro-electro-mechanical systems) sensors. In resonant mass sensing systems, a MEMS structure is oscillated at its resonant frequency and the shift in the resonant frequency is monitored to detect minute amounts of chemicals that bind on the sensor surface [1,2]. In atomic force microscopy, SSO has been implemented to perform tapping mode imaging [3,4]. MEMS cantilevers are commonly used in the above mentioned systems. In an SSO system that uses a cantilever as the mechanical structure, the oscillation frequency locks to the resonant frequency of the cantilever with the help of a feedback loop. The feedback loop amplifies the response of the cantilever, and adds certain amount of phase shift through a differentiation block before feeding the modified signal back to the cantilever. The feedback loop requires only a simple feedback electronics circuitry consisting of a differentiator and a variable gain amplifier to sustain the oscillation.

The SSO operation does not require an external AC signal generator to sweep the frequency in a pre-defined frequency range to find the resonant frequency. Thus, the main advantages of the SSO mode compared to the open loop or phase-locked loop (PLL) driven operations are mainly the simplicity of the electronics used and the possibility to parallelize the system easily due to this introduced simplicity.

MEMS and NEMS oscillator arrays can be fabricated with large number of elements but dense arrays cannot be interfaced easily to the actuation and read-out electronics. Therefore, array oscillators that share common actuator and common electronics are desirable for multi-channel sensor applications [5]. Recently, the parallel array operation has been demonstrated in Ref. [6] where we reported a sensor system that simultaneously oscillate and monitor an array of cantilevers using one actuator and one detector. The simultaneous SSOs of seven microcantilevers having different resonant frequencies within 65–120 kHz range operating in the air environment were demonstrated.

This paper focuses on the analysis of the SSO system and the theoretical limits, in order to maintain multiple oscillations. The

* Corresponding author.
E-mail address: uladiyan@ku.edu.tr (U. Adiyan).

http://dx.doi.org/10.1016/j.sna.2015.11.028
0924-4247/

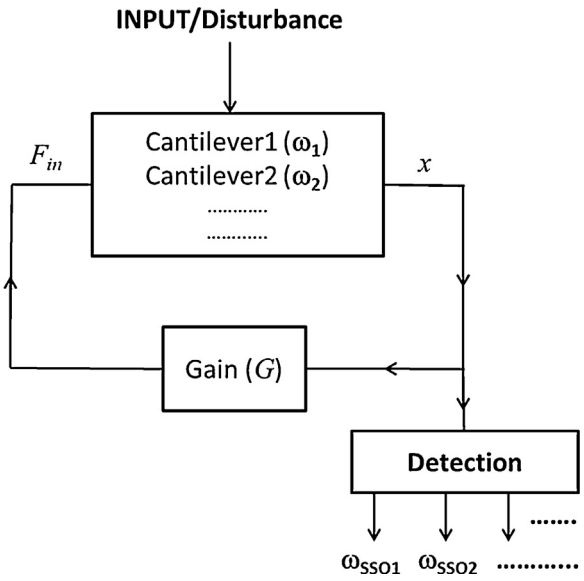

Fig. 1. The system block diagram of a sensor array operating in self-sustained oscillation mode.

theory of the SSO for a single cantilever case is well developed and reported previously [7–10]. However, the theory of the multi-cantilever SSO operation has not been visited until now to the best of our knowledge. The analysis of the multi-cantilever SSO is significant to understand the operation of the system, and it provides better and conscious designs by defining the operation limitations and specifications.

Section 2 gives the basic theory for two cantilever SSO systems. It discusses multiple oscillation criteria as well as cross coupling between the oscillators. The electrical and optical saturation mechanisms are introduced to the model. We showed that separate saturation mechanisms are required for each oscillator and this can be provided by using optical readout. Section 3 explains this nonlinear optical readout which is provided by diffraction gratings. Section 4 shows the modeling results and Section 5 shows experimental results for a two cantilever SSO system.

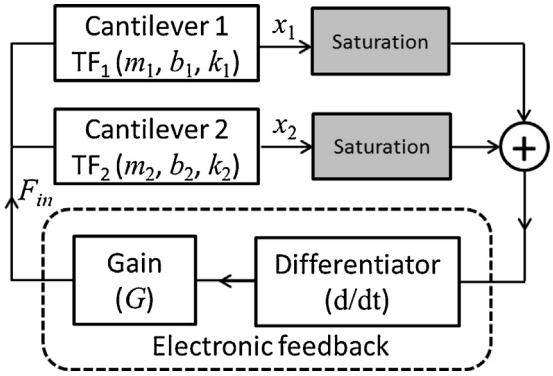

Fig. 2. Two cantilevers SSO block diagram with separate saturation blocks belonging to the each branch.

2. Analysis of the two-cantilever SSO

2.1. Sensor array oscillator operation

Fig. 1 shows block diagram overview of a sensor array using multiple cantilevers with SSO. The inputs can be biological, chemical or mechanical and the outputs are the oscillation frequencies of the cantilevers in the array. As it will be discussed in Section 2.2, different critical gain for each oscillator would be required for multiple cantilever SSO operation. This can be accomplished using different detector and amplifier for each cantilever. As we will show, if each cantilever has a different saturation mechanism and non-linearity only one detector can be sufficient which substantially simplifies the system for array oscillators.

2.2. Theory of the two-cantilever SSO

In an SSO system the closed-loop oscillation frequency locking is maintained by providing necessary gain and phase shift in the oscillation loop. For the sake of simplicity, "oscillation frequency" term will be used for the oscillating closed-loop system whereas "resonant frequency" term will be used for the cantilevers throughout the manuscript.

Fig. 2 shows the block diagram of the closed-loop two-cantilever SSO system which can be built using magnetically actuated nickel cantilevers and a nonlinear optical readout. One such implementation has been described in Ref. [11]. The cantilever displacements, x_1 and x_2, is detected by optical means and the actuation force, F_{in}, is created by an electro coil. The equation of motion of the two-cantilever system can be written starting with the transfer functions of the two cantilevers:

$$m_1\ddot{x}_1 + b_1\dot{x}_1 + k_1x_1 = F_{in} \tag{1}$$

and

$$m_2\ddot{x}_2 + b_2\dot{x}_2 + k_2x_2 = F_{in} \tag{2}$$

where $m_{1,2}$, $b_{1,2}$, $k_{1,2}$, are the effective masses, total damping's, spring constants, respectively. F_{in} depends on both responses of the first and the second cantilevers, i.e., x_1 and x_2 respectively; and also the feedback loop transfer function. F_{in} is:

$$F_{in} = G(\dot{x}_1 + \dot{x}_2) \tag{3}$$

In the Laplace domain, one can combine Eqs. (1)–(3) to find the characteristic equation:

$$m_1s^2 + b_1s + k_1 = Gs\left[1 + \frac{m_1s^2 + b_1s + k_1}{m_2s^2 + b_2s + k_2}\right] \tag{4}$$

Eq. (4) results in a 4th order polynomial. In general, there are 2 pairs of complex conjugate roots. If the roots have negative real

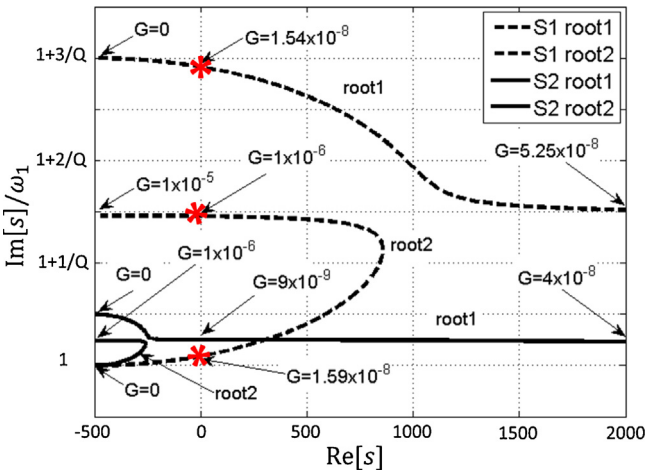

Fig. 3. The location of the roots of two cantilever SSO system when gain is swept from zero to 1×10^{-5}. S1 has the following properties $f1 = 100$ kHz, $f2 = 103$ kHz. Red stars indicate the SSO frequencies of S1. S2 has the following properties $f1 = 100$ kHz, $f2 = 100.5$ kHz. The Q and the spring constants of the cantilevers in both systems are 100 and 1 N/m, respectively.(For interpretation of the references to color in the text, the reader is referred to the web version of this article.)

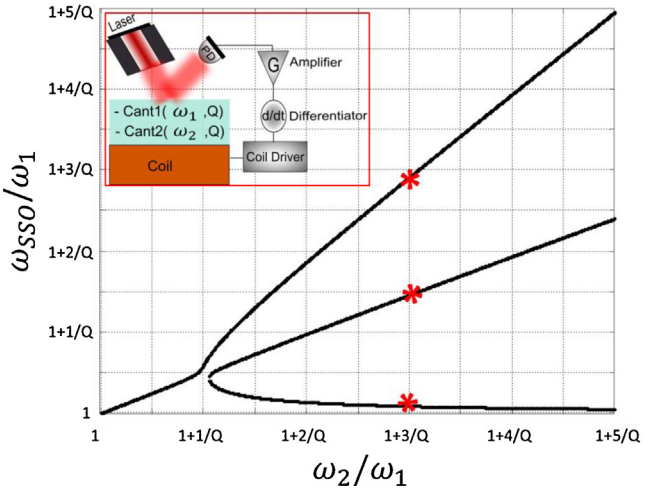

Fig. 4. The analytical solution of the equation of motion (4) of the two-cantilever SSO system. The cantilevers have two different resonant frequencies (ω_1, ω_2). Both axes are scaled by the frequency of low resonant cantilever (ω_1). ω_1 is assumed fixed and the High Resonant Frequency is varied (ω_2). Vertical axis shows the solutions of (4) for the two-cantilever SSO system (ω_{SSO}). Spring constants (=1 N/m) and the Q-factors ($Q = 100$) of cantilevers are assumed equal. Red stars show the SSO frequencies of S1 illustrated in Fig. 3.(For interpretation of the references to color in this figure legend, the reader is referred to the web version of this article.)

parts, the system results in exponentially decaying sinusoidal oscillations. For positive real parts, the system exhibits exponentially growing sinusoidal response. One can also plot the locations of the roots on the complex plane. The location of the roots on the complex plane is determined by the gain parameter (G) in the feedback. Therefore the gain parameter determines the nature of the response. In a special case where G is equal to the total damping of the system, s term in the characteristic equation vanishes and the solution has purely imaginary roots. However, in practice to sustain oscillations, it is not feasible to set the gain such that all the losses in the system are exactly compensated. Thus, by making the gain value a little above the critical value, it is possible to obtain diverging oscillations. These diverging oscillations stabilize at amplitude determined by the non-linearity, i.e., saturation mechanisms in the loop [10]. This non-linearity could be provided electrically, optically or even by mechanical means.

MATLAB was used to find the roots of the characteristic equation in (4). Fig. 3 shows the location of the roots on the complex plane where only the positive imaginary axis is considered. There are two systems depicted in the graph. The system S1 has two cantilevers with two different resonant frequencies where one cantilever has a resonance at $f1 = 100$ kHz and the second one has a resonance at $f2 = 103$ kHz while the second system S2 has two cantilevers with resonant frequencies at $f1 = 100$ kHz and at $f2 = 100.5$ kHz for the first and second cantilever respectively. The cantilevers in both systems (S1 and S2) are assumed to have the same $k = 1$ N/m and $Q = 100$. According to these system definitions, the difference between the resonances of the cantilevers in S1 is adjusted such that both roots intersect the imaginary axis where the real parts are zero, on the other hand only one root of S2 system intersects the imaginary axis. In S2 system, there is very little separation between the individual cantilever resonant frequencies. The roots of the characteristic equation (4) in order to obtain SSO are marked with red star marks. The star in the middle corresponds to the mutual oscillation frequency while the other two stars correspond to separate oscillation frequencies for different gain settings. Therefore, S1 will have potentially two distinct oscillation frequency in a closed loop system, whereas S2 will have only one oscillation frequency which is the average of the individual oscillation frequencies of the two cantilevers. Based on Fig. 3, one can calculate the oscillation frequencies and the required gain in a closed loop system. The minimum required gain is achieved when the real part is zero (i.e., poles are on the imaginary axis). We ran this calculation for a two-cantilever SSO system where we swept the resonant frequency of one of the cantilevers and calculated the oscillation frequency of the SSO while keeping the resonant frequency of the other cantilever constant. We assumed that the Qs and the spring constants of the cantilevers are the same, which is the case when arrays of cantilevers are fabricated on the same substrate with slightly changing lateral dimensions. Such arrays are used in resonant mass detection systems.

The inset image in Fig. 4 shows the basic model that is used for the calculation of SSO frequencies (ω_{SSO}) in a two-cantilever system with different resonant frequencies (ω_1, ω_2). According to the model, obtaining separate oscillations depend both on the resonant frequencies and the bandwidths of the cantilevers. If the resonant frequencies of the cantilevers are too close to each other (i.e., when the normalized high resonant frequency is in the range 1 and $1 + 1/Q$), the SSO system collapses into a single joint oscillation frequency. When the normalized high resonant frequency is greater than $1 + 1/Q$, there are three solutions of Eq. (4) as seen in Fig. 4. The SSO frequencies of the system S1 are indicated with red stars in Fig. 4 which corresponds to $1 + 3/Q$ in the x-axis. These three different oscillation frequencies lead to three different critical gain values as expected, which can be called as high, mutual, and low oscillation frequency critical gain values. The critical gain value belonging to the mutual oscillation frequency is always higher than the other two critical gain values (Fig. 3, 1.54×10^{-8} (corresponds to highest star in Fig. 4) and 1.59×10^{-8} (corresponds to lowest star in Fig. 4) for low and high resonances, 1.6×10^{-6} (corresponds to middle star in Fig. 4) for the mutual oscillation). Therefore, saturation mechanism becomes more of an issue in order to sustain multiple oscillations.

Basically, there can be two different saturation configurations in the SSO closed-loop system: either there is a single common saturation block in the feedback loop, or there are separate saturation mechanisms belonging to each oscillator, i.e., cantilever. When only one common single feedback saturation mechanism is employed, the overall loop gain of the system decreases to the lowest critical gain and sustained oscillations are obtained. Thus, the oscillation

frequency with the lowest critical gain can present in the system; whereas the other oscillation frequencies extinguish.

SSO system with separate saturation blocks belonging to each cantilever (shown in Fig. 2) can have different loop gains, and therefore it is possible to sustain two separate oscillation frequencies having different critical gains. Since the low and the high oscillation frequencies have lower critical gain values compared to the mutual oscillation frequency, two oscillation frequencies, which are sustained in the SSO system will be the low and the high oscillation frequencies. When the low (high) oscillation frequency sustain in its own branch, its effect on the other saturation block is degraded by the band-pass filtering effect of the high (low) resonance frequency oscillator. Thus, each saturation block is effectively saturated by the oscillation frequency supported by the cantilever in its branch.

Two main criteria are determined so far in order to have separate oscillation frequencies:

i Two resonant frequencies of the cantilevers should be separated by more than their 3 dB bandwidth BW = f/Q (i.e., the frequency spacing $\Delta f > \mathrm{BW}$ or more precisely $\Delta f > 0.5(\mathrm{BW}_1 + \mathrm{BW}_2)$).
ii Separate saturation mechanisms are needed for each cantilever.

Cantilevers are also used for biosensor applications in liquid environments. The resonant frequency differences between the cantilevers must be relatively large to make them operational, because the resonant frequencies and the damping can change considerably in liquid. For example, if 100 kHz resonant frequency cantilevers with Q of 100 are to be operated in liquid, the resonant frequency will drop to 30 kHz due to fluid damping (based on unpublished experimental data). The 3 dB bandwidth will also increase 10 times reducing the Q to 10. In this case, to sustain separate oscillations in an SSO system, one needs to design cantilevers to operate at 30 kHz and 33 kHz. Moreover, the other effects such as cross-coupling between the oscillators should be considered for biosensor applications.

2.3. Cross-coupling effect

The coupling between the oscillators has first come into consideration to describe the frequency effects of one oscillator on the second one operating at a close by frequency when electronic oscillators were built for microwave systems [12,13], and continues attracting attention, especially in radio frequency (RF) field [14,15]. Although it is mostly investigated for RF systems, the phenomenon can be observed in any system that involves coupled oscillators, such as the cantilever systems considered here. Therefore, the changes in the resonance of one cantilever will affect the oscillation frequency of the other cantilever as shown in Fig. 4.

Fig. 5 shows the amount of cross-coupling between two cantilevers as one of the resonances (ω_2) increased while ω_1 is kept constant. As expected, as the frequency separation increases cross coupling decreases. If the separation between the normalized resonant frequencies is higher than 5BW the cross coupling drops less than 1% i.e., if one of the resonances shifts 1 Hz, the other resonance will shift less than 0.01 Hz. This cross-coupling leads to another phenomenon called as frequency pulling effect. When the two cantilevers are oscillated at the same time, there will be slight changes in the frequencies of the oscillators. This frequency pulling can be investigated by considering the open-loop frequency response of the system shown in Fig. 2, from F_{in} to the input of the differentiator stage.

Fig. 6 shows the open loop responses of individual cantilevers as well as the total response. These graphs can be used to explain the cross-coupling mechanism as well as the frequency pulling when two cantilevers are operated in the same SSO system. According to

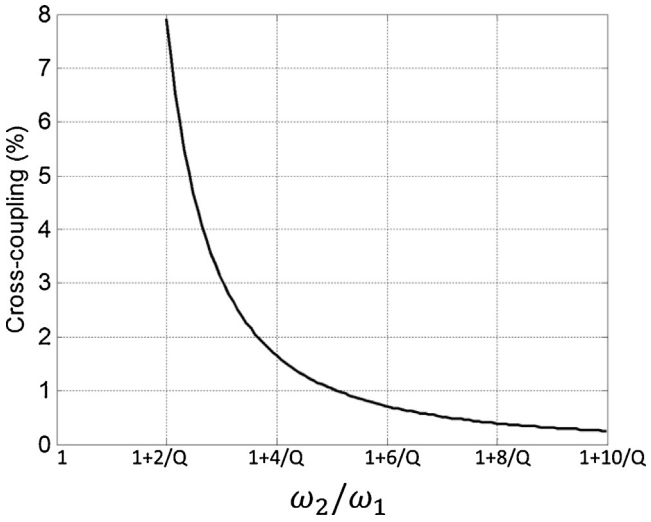

Fig. 5. Cross-coupling between the SSO frequencies of two cantilevers oscillating in an SSO system. This figure shows the change in the oscillation frequency of the cantilever with low SSO frequency due to a change for the cantilever with high resonant frequency.

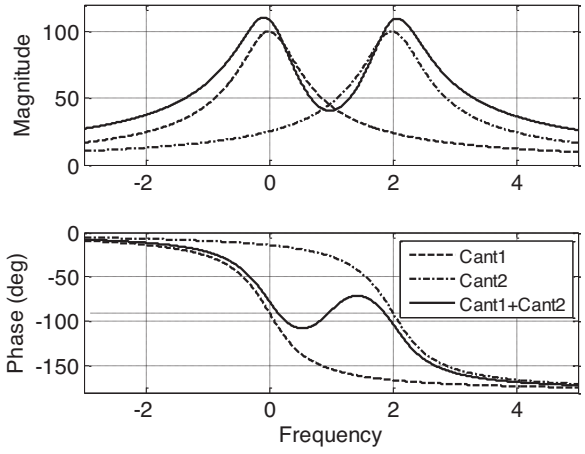

Fig. 6. The amplitude and phase transfer functions of the two cantilevers and the total response. Frequency axis is normalized by the low resonant frequency and the bandwidth. −90° line is also added to the lower graph.

the total response calculation, the resonant frequency where the phase is 90° moves toward the average of the individual resonant frequencies. In the closed loop system, the cantilevers will oscillate at the frequencies determined by the combined phase curve. When the resonant frequencies of oscillators are too close to each other, both oscillators oscillate at a mutual frequency through which is called injection locking . If the resonant frequencies are well separated then they affect each other slightly. This is called injection pulling.

According to the derived solution, cross-coupling between two cantilevers can be calculated, and the sensor output can be corrected in view of the above.

3. Non-linear optical readout

It's been already mentioned that saturation mechanism is vital for oscillators. In addition to this, we already discussed that separate saturation mechanisms are needed in an effort to sustain multiple oscillations. The electrical non-linearity can be an example of common single saturation whereas both the mechanical and optical non-linearities can be the examples of separate sat-

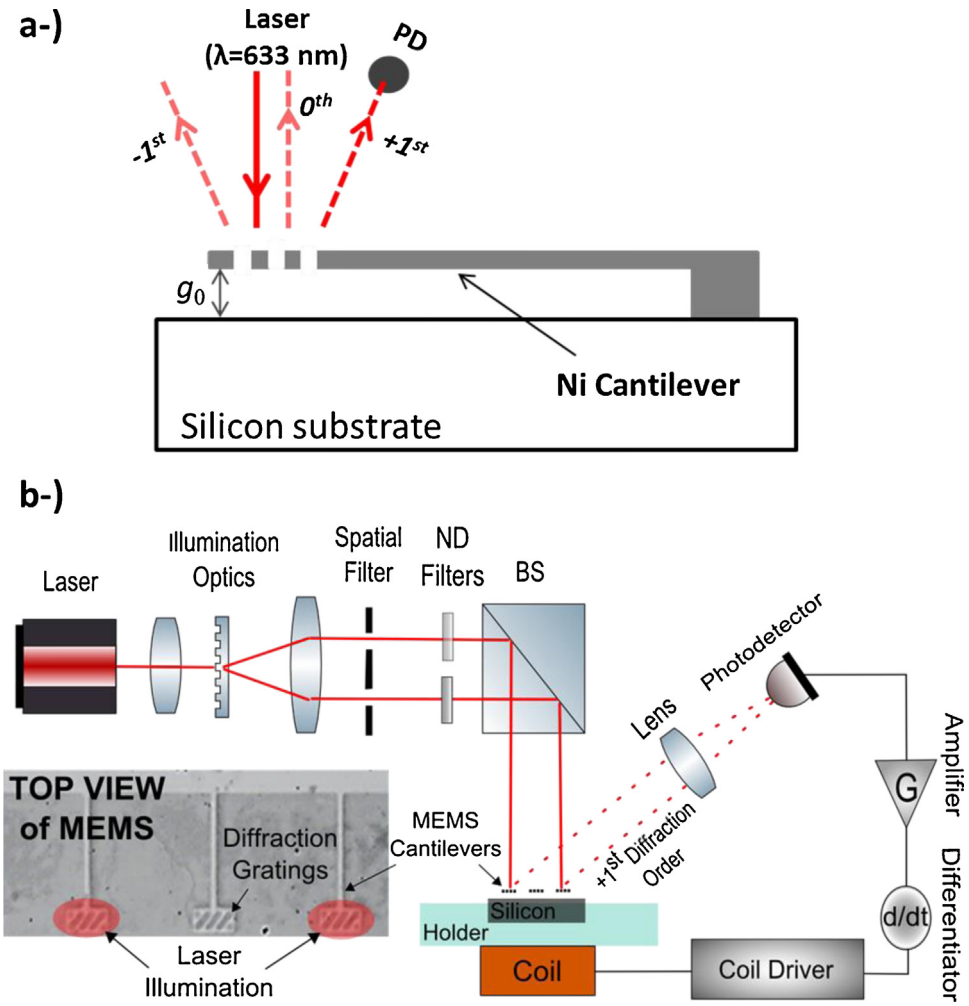

Fig. 7. (a) Cross-section of a cantilever with an integrated diffraction grating. 0th and ±1st diffraction orders are shown. A photodiode (PD) is used to monitor the +1st diffraction order. (b) The system overview of the nonlinear optical readout of the two-cantilever SSO system. Neutral density (ND) filter to attenuate and equalize outputs of channels; spatial filter: two square openings to select the desired cantilevers. Inset shows top view of a cantilever array overlaid with laser illumination area.

uration mechanisms for the MEMS cantilever based sensor array system. Consequently, we can use either mechanical or optical non-linearities for the purpose of having separate saturation mechanisms with a single feedback loop. The mechanical saturation depends only on the deflection amplitude and the mechanical properties of the cantilever, and it can be observed when the deflection values are high enough to create non-linearity. But for our case, the operating points of the cantilevers are far away from the mechanical saturation, which makes it unfeasible to use mechanical saturation to sustain multiple oscillations in the SSO system.

In view of the above, the desired saturation mechanism can be generated using a diffraction grating based optical readout as shown in Fig. 7. Fig. 7a shows the cross-section of a single cantilever with diffraction gratings. In Fig. 7b, the system overview with a detailed illustration of the optical readout setup is given. The actuation of the cantilevers is achieved by using an electro coil which provides an alternating magnetic field that will drive the cantilevers at their resonant frequencies. The coil is placed underneath the cantilevers along with a set of magnets [11]. The interferometric readout is based on the optical path difference (OPD) between the reflected light from the diffraction grating integrated MEMS cantilever surface and from the substrate underneath the cantilever array [6,11,16]. The OPD of the incident beam is twice the sum of the initial gap underneath the cantilever and the deflection amplitude of the cantilever. The non-linear characteristic of the interferometric readout is explained as:

$$I = B\sin^2\left(\frac{2\pi}{\lambda}d\right) = \frac{B}{2} - \frac{B}{2}\cos\left(\frac{4\pi}{\lambda}d\right) \tag{5}$$

where I is the intensity, B is the constant amplitude depending on the gain of the photodetector and laser power, λ is the wavelength of the readout laser beam, and d is the varying gap with respect to time, which can be written as:

$$d = g_0 + A\sin(\omega_0 t) \tag{6}$$

where g_0 is the initial gap underneath the MEMS cantilever when there is no deflection, A is the deflection amplitude, and ω_0 is the deflection oscillation frequency.

Fig. 8 shows the calculated and experimental interferometric response curve based on the intensity of the +1st diffraction order with respect to gap for the grating readout. In the experiment, a magnet was placed under the MEMS cantilevers and the magnetic field deflected the cantilever toward the substrate and the initial gap changed. The selected cantilever was illuminated with a red laser (λ = 633 nm). The amplitude of the +1st diffracted order from the grating was measured while moving the magnet using a precision translation stage. The magnetic field was also measured using a Tesla-meter. We calibrated these measurements by measuring the actual displacement of the cantilever under white light

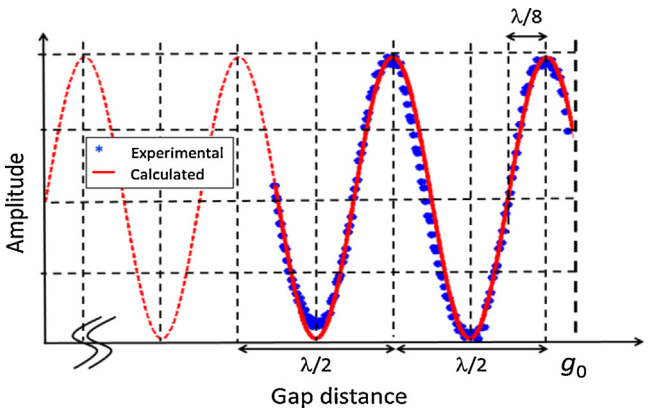

Fig. 8. Interferometric response curve according to the calculated and the experimental data. Experimental data is obtained by moving a super strong magnet from the closest point to the cantilevers to a farther location. g_0 shows the nominal gap between the cantilever and the substrate. Gaps those are different from the nominal value results in reduced sensitivity.(For interpretation of the references to color in the text, the reader is referred to the web version of this article.)

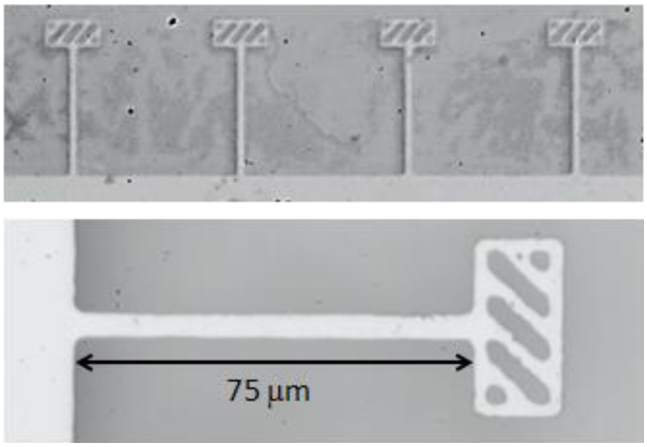

Fig. 9. Nickel cantilevers were used in the experiments. The thickness is 2 μm. Top picture shows a portion of a cantilever array. Bottom picture is the zoomed view of one of the cantilevers.

interferometer for a given magnetic field. Then the measured intensity values are plotted with respect to the gap distance which is transformed from the recorded magnetic fields. There is a good agreement between the experimental and calculated data. As it can be seen from this, the interferometric response curve is the saturation mechanism which limits the oscillation amplitude due to the optical nonlinearity. This sinusoidal nonlinearity provides the separate saturation mechanisms from the diffraction gratings needed for each cantilever. Thereby, each oscillator has its own loop gain and oscillation frequency independent from the other oscillators in the array.

4. System simulation results

MEMS based cantilever array SSO system with two cantilevers is modeled using MATLAB Simulink. System analyses are performed firstly using two cantilever sensor model with a common electronics saturation block. Secondly same cantilever model is used with separate saturation blocks by means of nonlinear optical readout.

Several cases were investigated as shown in Table 1. The frequency of 1st cantilever was fixed at 100 kHz while the frequency of 2nd cantilever was varied. We also assumed the 3 dB bandwidth as 1 kHz for both cantilevers. Table 1 lists the cantilever resonant frequencies and the resulting simulated oscillation frequencies in the system.

The simulation results listed in Table 1 lead to the following conclusions, which also support the analytical findings of Section 2 of this paper including the single and multiple SSO frequencies and the cross-coupling effect between the cantilevers:

- Case 1, 2, 3: It is possible to sustain multiple SSO, if the resonant frequency difference is greater than the 3 dB BW. This is enabled by having separate saturation mechanism in each branch.
- Case 4: The system oscillates at the resonant frequency of the oscillator with the lower critical gain with a slight shift due to frequency pull of the other cantilever. Thus, two oscillation frequencies cannot be observed even though the two resonances are well separated. This is due to the common saturation mechanism employed in this case.
- Case 5: There is only a single mutual oscillation in the system, as the resonant frequency difference is lower than the 3 dB BW.

5. Experimental results

In the experiments, we used nickel cantilevers with integrated diffraction gratings. Fig. 9 shows optical microscope pictures of the cantilevers. The fabrication procedures of the cantilevers can be found elsewhere [6,11]. The resonant frequencies of these cantilevers were around 20 kHz in air.

In the experiments, the cantilevers were illuminated by a red laser which wavelength is 633 nm. During cantilever fabrication, the gap between the grating and the substrate was set to obtain maximum sensitivity as described in Fig. 8. If one can set the gap g_0 to $n\lambda/2+\lambda/8$ where n is an integer number, the grating operates with maximum sensitivity. However, fabrication non-uniformities affected the gap. Therefore, the sensitivity of each cantilever was slightly different depending on where the grating operates in the non-linear response curve as indicated between $g_0-\lambda/8$ and $g_0+\lambda/8$. As shown in Fig. 7b, we added neutral density filters (attenuator) on the laser beam path to approximately equalize the optical output of the cantilevers, and a spatial filter consisting of two square openings to illuminate the desired cantilevers. The cantilevers were vibrated by an AC magnetic field generated by an electro magnet (coil). While obtaining frequency scans, we kept the drive current for the coil small enough to operate the grating at its linear region. However, we confirmed (using a laser Doppler vibrometer) that the oscillation amplitudes were around 160 nm ($\lambda/4$) peak-to-peak at the tip of the cantilevers for the SSO systems. This confirms that the amplitude is limited by the optical non-linearity, not by the coil drive current.

To demonstrate Case 5 of Table 1, we selected two cantilevers with resonant frequencies that were very close to each other. The individual frequency responses of the cantilevers are shown in Fig. 10. The gain of the feedback electronics were increased until an oscillation was achieved. Cantilever SSOs were observed one at a time by blocking the light diffracted from the other cantilever and subsequently they were observed simultaneously without changing the gain and phase settings.

Resonant frequencies and quality factors are summarized in Table 2. The oscillation frequencies for individual cantilevers (f_1 and f_2) are given in the 4th row of the table. The cantilevers do not oscillate exactly at the peak amplitude of the resonance curve due to the additional phase errors that may exist in the electronics. Nevertheless, when both cantilevers are oscillated in the same closed loop system, rather than two oscillations, there exists only one oscillation at a frequency (f_3) between f_1 and f_2 which is due to the resonant frequency separation which is smaller than

Table 1
Resonance and corresponding oscillation frequencies of the two-cantilever SSO system for changing dominant saturation mechanisms.

Case	1st cant. res. freq. (kHz)	2nd cant. res. freq. (kHz)	Dominant Sat. Mech.	System Osc. Freq. (kHz)	
1	100	105	Optical & separate	100.04	104.96
2	100	102	Optical & separate	100.11	101.87
3	100	101	Optical & separate	100.36	100.62
4	100	105	Electrical & common	Single osc. (~100 or ~105)	
5	100	100.5	Optical & separate	100.25	
6	100	100.5	Electrical & common	100.25	

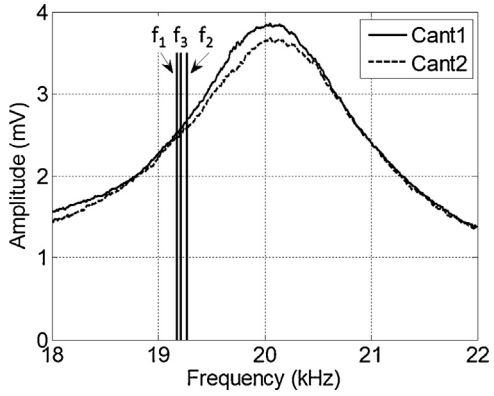

Fig. 10. Frequency response of two cantilevers that have very similar resonant frequencies. Oscillation frequencies (f_1–f_3) from Table 2 are also added to the figure.

Table 2
Resonances and corresponding oscillation frequencies of the two-cantilever SSO where individual resonances are very close.

	Cant1	Cant2
Amplitude peak	20.051 kHz	20.055 kHz
BW (Q)	1.5 kHz (13.37)	1.61 kHz (12.38)
Separate SSO	19.176 kHz (f_1)	19.264 kHz (f_2)
Both SSO	19.216 kHz (f_3)	

$\Delta f < 0.5(BW_1 + BW_2)$. When the two cantilevers are involved in the closed loop system, both SSO frequency (f_3) should be in the middle of f_1 and f_2 according to the theory. Experimentally determined "both SSO" frequency (f_3) confirms the theory with a small error (due to the phase shift in the electronics) that we outlined in Section 2 and the simulation results in Section 4.

We also experimented with cantilevers where there was a larger separation in the resonant frequencies. The selection of the cantilevers aligns with Cases 1, 2, 3 of Table 1. We repeated the same procedure to oscillate the cantilevers. We increased the gain until we observed two oscillations. The spectra of the individual cantilever and two cantilevers SSO's are given in Fig. 11.

The individual frequency sweeps of the cantilevers are given in Fig. 12 along with the oscillation frequencies of the SSO systems. As before, the cantilevers do not oscillate at the peaks of their resonance curves due to the additional phase errors that may exist in the electronics. Same phase and gain settings were used in all measurements. The resonance properties are summarized in Table 3. The individual oscillation frequencies (f_1 and f_2) of the cantilevers in an SSO system are 19.6 kHz and 21.617 kHz. When both cantilevers oscillated in the SSO, the oscillation frequency corresponding to the cantilever with low resonant frequency (f_3) increased by 185 Hz and the oscillation frequency of the other cantilever (f_4) reduced by 90 Hz which is an experimental observation for injection pulling. According to the theory outlined in Section 2, since the resonant frequencies of the two cantilevers are separated larger than 0.5(BW1 + BW2), one should observe two separate oscillations in the closed loop system. The separate SSO frequencies (f_1 and f_2) should get closer to each other in a closed loop system which exhibits the both SSO frequencies (f_3 and f_4). The magnitudes of these shifts are difficult to estimate using the model that we developed because of the additional phase errors in the electronics but the behavior is consistent with the simulations.

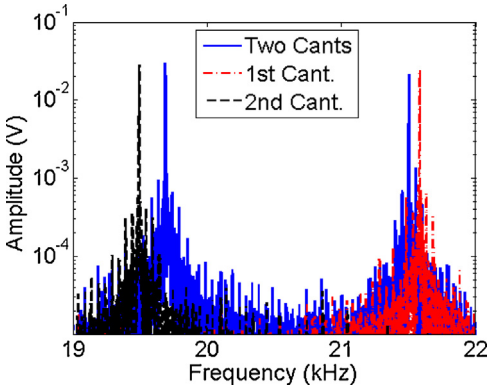

Fig. 11. Spectra of SSO system when individual cantilevers and both cantilevers are oscillated. The individual oscillations were obtained by selectively blocking the light diffracted from the cantilevers.

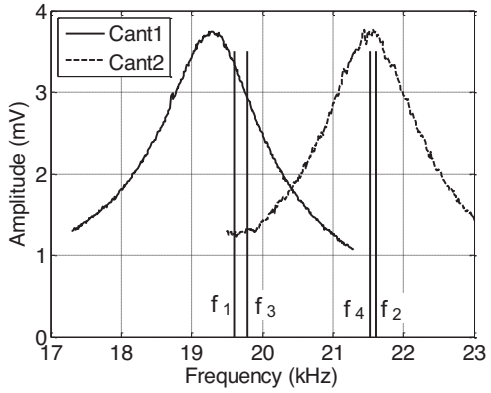

Fig. 12. Frequency response of two cantilevers that have resonances further away from each other. Oscillation frequencies (f_1–f_4) from Table 3 are also added to the figure.

Table 3
Resonances and corresponding oscillation frequencies of the double cantilever SSO where individual resonances are further away.

	Cant1	Cant2
Amplitude peak	19.325 kHz	21.577 kHz
BW (Q)	1.301 kHz (14.85)	1.234 kHz (17.48)
Separate SSO	19.600 kHz (f_1)	21.617 kHz (f_2)
Both SSO	19.785 kHz (f_3)	21.527 kHz (f_4)

6. Conclusion

This work provides an analysis and modeling of two cantilevers oscillated at resonance with common actuator and a single feedback circuitry. To sustain multiple oscillations two main criteria are established: (i) a frequency spacing Δf greater than 3 dB bandwidth (BW) is required between their resonant frequencies. Otherwise the system collapses into a single oscillation; (ii) separate saturation mechanisms are needed for each oscillator, which is achieved using the diffraction grating based optical readout in our system. Experimental results matched well with the theory and the simulations. The analysis in this paper can be extended into large number of cantilevers operated in the same loop using common actuator and feedback electronics. However, there are limitations: the change in one oscillator induces a change in the other oscillator. This cross-coupling effect between the cantilevers can be determined and corrected for a sensor application. Finally, to achieve high performance and low cross-coupling sensor arrays, high Q-factor and large separation between oscillator frequencies are desired (e.g., $\Delta f = 5$ BW results in <1% cross coupling).

Acknowledgments

This project is partly sponsored by TUBITAK grants 113S074 and 111E184.

References

[1] N.V. Lavrik, M.J. Sepaniak, P.G. Datskos, Cantilever transducers as a platform for chemical and biological sensors, Rev. Sci. Ins. 75 (2004) 2229–2253.
[2] J.L. Arlett, E.B. Myers, M.L. Roukes, Comparative advantages of mechanical biosensors, Nat. Nanotechnol. 6 (2011) 203–215.
[3] M. Basso, P. Paoletti, B. Tiribilli, M. Vasalli, Modelling and analysis of auto-tapping AFM, 47th IEEE Conference on Decision and Control (2008) 5188–5193.
[4] L. Manning, B. Rogers, M. Jones, J.D. Adams, Self-oscillating tapping mode atomic force microscopy, Rev. Sci. Ins. 74 (9) (2015) 4220–4222.
[5] O. Cakmak, E. Ermek, N. Kilinc, S. Bulut, I. Baris, I. Kavakli, et al., A cartridge based sensor array platform for multiple coagulation measurements from plasma, Lab Chip 15 (2015) 113–120.
[6] S.Z. Lulec, C. Sagiroglu, A. Mostafazadeh, E. Ermek, E. Timurdogan, Y. Leblebici, et al., Simultaneous self-sustained actuation and parallel readout with MEMS cantilever sensor array, in: 25th International Conference on Micro Electro Mechanical Systems (MEMS), IEEE Paris, France, 2012, pp. 644–647.
[7] M.G. Muriuki, W.W. Clark, Q.M. Chen, Q.M. Wang, Design and analysis of a piezoelectric cantilever beam resonator, Proceeding SPIE Smart Structures and Materials: Smart Electronics, MEMS, BioMEMS, and Nanotechnology 5055 (2003) 36–47.
[8] J.D. Adams, G. Parrott, C. Bauer, T. Sant, L. Manning, M. Jones, B. Rogers, D. McCorkle, T.L. Ferrell, Nanowatt chemical vapor detection with a self-sensing, piezoelectric microcantilever array, Appl. Phys. Lett. 83 (2003) 3428–3430.
[9] B. Rogers, L. Manning, M. Jones, T. Sulchek, K. Murray, B. Beneschott, J.D. Adams, Z. Hu, T. Thundat, H. Cavazos, S.C. Minne, Mercury vapor detection with a self-sensing, resonating piezoelectric cantilever, Rev. Sci. Ins. 74 (2003) 4899–4901.
[10] M. Basso, P. Paoletti, B. Tiribilli, M. Vasalli, Modelling and analysis of autonomous micro-cantilever oscillations, Nanotechnology 19 (2008) 475501.
[11] A. Ozturk, H.I. Ocakli, N. Ozber, H. Urey, I.H. Kavakli, B.E. Alaca, A magnetically actuated resonant mass sensor with integrated optical readout, IEEE Photonics Technol. Lett. 20 (2008) 1905–1907.
[12] R. Adler, A study of locking phenomena in oscillators, Proc. IEEE 61 (1973) 1380–1385.
[13] H.L. Stover, Theoretical explanation of the output spectra of unlocked driven oscillators, Proc. IEEE 54 (1966) 310–311.
[14] B. Razavi, A study of injection locking and pulling in oscillators, IEEE J. Solid-State Circuits 39 (2004) 1415–1424.
[15] S. Sancho, M. Ponton, A. Suarez, F. Ramirez, Analysis of injection pulling in phase-locked loops with a new modeling technique, IEEE Trans. Microwave Theory Tech. 61 (2013) 1200–1214.
[16] G.G. Yaralioglu, A. Atalar, S.R. Manalis, C.F. Quate, Analysis and design of an interdigital cantilever as a displacement sensor, Appl. Phys. Lett. 83 (1988) 7405–7415.

Biographies

Sevil Zeynep Lulec received the B.S. degree in electrical and electronics engineering from METU, Ankara, Turkey, in 2008 and the M.S. degree in the same field from EPFL, Lausanne, Switzerland, in 2010. She is currently pursuing the PhD. degree in electronics engineering at the University of Toronto, Canada. From 2010 to 2011, she was a Research Engineer in Koc University Optical Microsystems Laboratory. From 2011 to 2012 she worked as a Scientific Project Expert in METU-MEMS Research and Application Center. Her research interests include analog and mixed signal IC design, MEMS modeling, and plasmonic integrated IR imaging. Mrs. Lulec is a recipient of EPFL Excellence Scholarship in between 2008 and 2010 and the ADI Outstanding Student Designer Award in 2013.

Ulas Adiyan received the B.Sc. degree from Istanbul Technical University (ITU), Turkey, in 2007, in Telecommunication Engineering and M.Sc. degree in Electronics and Communication Engineering from the same university in 2010. He is a PhD. candidate in Electrical and Electronics Engineering Department in Koç University. He is currently a member of OML Research Group where he is currently studying thermo-mechanical IR MEMS detectors. His research interests include development of micro-opto-mechanical systems.

Goksen G. Yaralioglu received his B.Sc., M.Sc., and PhD. degrees from Bilkent University, Ankara, Turkey, in 1992, 1994, and 1999, respectively, all in electrical engineering. He is now working as an Associate Professor in the Electrical and Electronics Engineering Department, Ozyegin University, Istanbul, Turkey. His current research interests include design, modeling and applications of micromachined ultrasonic transducers, atomic force microscopy at ultrasonic frequencies, microfluidic channels, MEMS sensors and inertial sensors.

Yusuf Leblebici received the B.Sc. and M.Sc. degrees in electrical engineering from Istanbul Technical University, Istanbul, Turkey, in 1984 and 1986, respectively, and the PhD. degree in electrical and computer engineering from the University of Illinois at Urbana-Champaign, in 1990. Since 2002, he is a Chair Professor at the Swiss Federal Institute of Technology in Lausanne (EPFL) and the Director of the Microelectronic Systems Laboratory. His research interests include design of high-speed CMOS digital and mixed-signal integrated circuits, computer-aided design of VLSI systems, intelligent sensor interfaces, modeling and simulation of semiconductor devices and VLSI reliability analysis. He is the coauthor of six textbooks, as well as more than 300 articles published in various journals and conferences. Dr. Leblebici has served as an Associate Editor of the IEEE Transactions on Circuits and Systems (TCAS-II) and IEEE Transactions on Very Large Scale Integrated (VLSI) Systems. He has been elected as Distinguished Lecturer of the IEEE Circuits and Systems Society for 2010/2011.

Hakan Urey received the B.Sc. degree from Middle East Technical University, Ankara, in 1992, and M.Sc. and PhD. degrees from Georgia Institute of Technology in 1996 and in 1997, all in Electrical Engineering. After completing his PhD., he joined Microvision Inc.,-Seattle as Research Engineer and he played a key role in the development of the Retinal Scanning Display technology. He was the Principal System Engineer when he left Microvision to join the faculty of engineering at Koç University in 2001. He was promoted to Associate Professor in 2007 and Professor in 2010. He published about 50 journals and 100 international conference papers, 7 edited books, 4 book chapters, and has more than 25 issued and several pending patents. His research interests are in the area of optical MEMS, micro-optics and optical system design, 2D/3D display and imaging systems, and biosensors. He is a member of SPIE, IEEE, and OSA. He received an Advanced grant from the European Research Council (ERC-AdG) in 2013, Outstanding Faculty Award from Koç University in 2013, TÜBITAK-Encouragement Award in 2009, Outstanding Young Scientist Award from the Turkish Academy of Sciences (TÜBA) in 2007, and Werner Von Siemens Excellence Award in 2006.